Comparison on the Scattering Path Loss of Terahertz Waves in Fat Layer Under Air-Enclosed and Tissue-Enclosed Conditions

Zoha Ameri and Fazel Jahangiri*

Laser and Plasma Research Institute, Shahid Beheshti University, Evin, Tehran, Iran

***Corresponding author email:** f_jahangiri@sbu.ac.ir

Regular paper: Received: Oct. 27, 2022, Revised: Feb. 04, 2023, Accepted: Feb. 04, 2023,
Available Online: Feb. 06, 2023, DOI: 10.52547/ijop.16.2.139

ABSTRACT— Using terahertz waves for intra-body communications between nanomachines is associated with dissipation during propagation, of which scattering is one of the most important effects. In this paper, scattering path loss with two different assumptions of air-enclosed and tissue-enclosed in subcutaneous fat is calculated and compared. The results show that for TM polarization, air-enclosed assumption gives smaller and greater scattering loss for frequencies less and bigger than 0.26 THz. The greatest difference between air-enclosed and tissue-enclosed results is observed for TE polarization at the approximate frequency of 0.4 THz.

KEYWORDS: Scattering Path Loss, Terahertz, Intra-Body Wireless Communications

I. INTRODUCTION

Terahertz waves occupy the frequency range of 0.1-10 THz in the electromagnetic spectrum. Interesting features of terahertz waves have motivated numerous applications of this radiation in various fields [1]. Terahertz radiation could provide spectrum fingerprint for various materials, and terahertz spectroscopy have been utilized for material inspection in industry, security and medical applications [2]. Despite its high penetration depth, it consists of low energy photons without ionizing effects, which makes it a suitable candidate for safe medical imaging and spectroscopy purposes [3]. Moreover, different materials yield distinct spectroscopic behaviors in terahertz frequency region due to their rotational transitions therefore conductors are reflective and bipolar materials are absorptive [4]. The spectral response of biological samples' water content to terahertz radiation has attracted much attention, especially in medical applications [3]. In addition, broadband terahertz wave with high reliability, energy efficiency, and transfer rate, has found its place in wireless communications [5]. Despite absorption and spreading path loss, scattering has gained little attention in the literature. However, in the It has been anticipated that this frequency range can be applied in cellular mobile communications, space communications and intrabody communications. Wireless communication could be enabled between nanomachines embedded inside the human body for real-time health monitoring followed by drug delivery. Nano-machine is an integrated nano-devices with the size of 10-100 μm^2, which is able to detect and measure events in the scale of nanometers. Since measurement in micro scale is required for medical purposes, multiple nanomachines are connected as a nanonetwork with micrometer scale performance [6]. Therefore, a nanomachine should be equipped by a wireless communication unit. In fact, a nanomachine consists of at least six general parts: 1. Nanosensor, 2. Nanoactuator, 3. Nanopower, 4. Nanoprocessor, 5. Nanomemory, and 6. Nanocommunication. After collecting information in the body, these nanomachines transfer the data to an external receiver (such as a wearable device) [7].

[Downloaded from ijop.ir on 2026-11-25]

For wireless electromagnetic communication between nanomachines, three frequency regions of radio, optical, and terahertz have been proposed. However, radio frequency is associated with large nanomachine size, high complexity, and substantial power consumption. Moreover, although optical frequency has a higher achievable data rate, accuracy, and safety, in comparison with radio frequency, it cannot surpass terahertz range in terms of nanomachine design. Recently, tunable nano-antenna construction with appropriate size and power has become possible via graphene derivatives that operate in the terahertz band [8]. Therefore, terahertz wave has been proposed as a proper frequency range for enabling intra-body nanomachines communications [9]. The propagation inside the body and between human tissues is associated with different path losses such as absorption, spreading, and scattering. Despite absorption and spreading path loss, scattering has gained little attention in the literature. However, in the recent years scattering along with absorption and spreading path losses have been surveyed for water, skin and blood in the frequency range of 0.1-1 THz [10].

We have recently taken into account Rayleigh scattering of epidermis, dermis and blood tissue for tissue-enclosed and air-enclosed conditions in the terahertz frequency range by considering the particle's shape, size and refractive index differences [11]. In tissues like blood, scattering of most cells falls in the Rayleigh region which makes scattering neglectable in comparison with absorption and spreading losses. However, in tissues such as fat with cell diameters of 50-150 micrometers, scattering can be substantial.

One of the important parameters in determining the intensity of scattering is the refractive index contrast between particle and its surrounding medium. Usually in scattering analysis even in the case of in-vivo scattering, only tissue's refractive index is considered [10]. Which indicates the assumption of air as the surrounding medium (air-enclosed case). However, this assumption can result in an overestimation or underestimation of intra-body scattering path loss calculations. In this paper, the scattering path loss of fat tissue with two assumptions of: 1. The propagation of terahertz wave in the air and its collision with fat tissue (air-enclosed case) and 2. The scattering of terahertz wave in fat tissue due to its collision with fat cells embedded in a mesh of collagens (tissue-enclosed case) have been compared.

In the air-enclosed case, air is the surrounding medium whereas in the tissue-enclosed one, collagen type I is considered the ambient medium. The first step for calculating scattering is the calculation of frequency-dependent refractive index via the electric permittivity. In this regard, by considering the high-water percentage in collagen tissue and also by taking into account the accuracy of the Double-Debye (d-Debye) model for polar liquids, Double-Debye model is used for the calculation of collagen's refractive index. On the other side, by taking into consideration the trivial water percentage in fat tissue, the double-Cole-Cole (d-Cole-Cole) model is instead used for the calculation of fat tissue's refractive index. Since in the case of tissue-enclosed scattering the contrast of refractive indices is small and the particle size condition is satisfied, Rayleigh-Gans-Born (RGB) model is utilized.

Table **1**: Scattering Regimes Conditions

Particle Size $\left(x = ka = \frac{2\pi a}{\lambda}\right)$	Relative refractive index $\left(m = \frac{n_{scat.}}{n_{en.-med.}}\right)$	Scattering Regime
$2x\lvert m-1\rvert \ll 1$	$\lvert m-1\rvert \ll 1$	Rayleigh-Gans-Born
Arbitrary	Arbitrary	Mie

For air-enclosed scattering, the accurate Mie model is used. Regardless of having less accuracy in comparison with Mie model, Rayleigh-Gans-Born model provides suitable results especially in the second half of surveyed region. The mentioned scattering regimes conditions are summarized in Table 1, in which x is the size parameter, a is the radius of the scatterer, m indicates the relative refractive index, k denotes the wavenumber, λ is the wavelength, and n_{scat} and n_{en-med} are the

[Downloaded from ijop.ir on 2026-11-25]

refractive index of the scatterer and its enclosed medium, respectively.

II. Modeling of Scattering Path Loss

The d-Debye model and its real and imaginary parts are denoted in Eqs. 1-3. In these equations, ε_1, ε_2 and ε_∞ are static, intermediate, and high-frequency limit permittivities respectively. ω is the angular frequency and, τ_1 and τ_2 are the slow and fast relaxation times [12].

$$\varepsilon(\omega) = \varepsilon_\infty + \frac{(\varepsilon_1-\varepsilon_2)}{1+i\omega\tau_1} + \frac{(\varepsilon_2-\varepsilon_\infty)}{1+i\omega\tau_2} \quad (1)$$

$$\varepsilon' = \varepsilon_\infty + \frac{(\varepsilon_1-\varepsilon_2)}{1+(\omega\tau_1)^2} + \frac{(\varepsilon_2-\varepsilon_\infty)}{1+(\omega\tau_2)^2} \quad (2)$$

$$\varepsilon'' = \frac{(\varepsilon_1-\varepsilon_2)\omega\tau_1}{1+(\omega\tau_1)^2} + \frac{(\varepsilon_2-\varepsilon_\infty)\omega\tau_2}{1+(\omega\tau_2)^2} \quad (3)$$

The d-Cole-Cole equation together with its real and imaginary parts are shown in Eqs. 4-6. Debye model modifies to Cole-Cole with the addition of α parameter ($0 < \alpha < 1$). This parameter can be a measure of the broadness of dispersion region [13]. With α_1, $\alpha_2 = 0$, double-Cole-Cole model converges to double-Debye model.

$$\varepsilon(\omega) = \varepsilon_\infty + \frac{(\varepsilon_1-\varepsilon_2)}{1+(i\omega\tau_1)^{1-\alpha_1}} + \frac{(\varepsilon_2-\varepsilon_\infty)}{1+(i\omega\tau_2)^{1-\alpha_2}} \quad (4)$$

$$\epsilon' = \varepsilon_\infty + (\varepsilon_1 - \varepsilon_2) \times \times \frac{1+(\omega\tau_1)^{1-\alpha_1}\sin\left(\frac{\alpha_1\pi}{2}\right)}{1+2(\omega\tau_1)^{1-\alpha_1}\sin\left(\frac{\alpha_1\pi}{2}\right)+(\omega\tau_1)^{2(1-\alpha_1)}} + (\varepsilon_2 - \varepsilon_\infty)\frac{1+(\omega\tau_2)^{1-\alpha_2}\sin\left(\frac{\alpha_2\pi}{2}\right)}{1+2(\omega\tau_2)^{1-\alpha_2}\sin\left(\frac{\alpha_2\pi}{2}\right)+(\omega\tau_2)^{2(1-\alpha_2)}} \quad (5)$$

$$\varepsilon'' = \frac{(\varepsilon_1-\varepsilon_2)(\omega\tau_1)^{1-\alpha_1}cos\left(\frac{\alpha_1\pi}{2}\right)}{1+2(\omega\tau_1)^{1-\alpha_1}\sin\left(\frac{\alpha_1\pi}{2}\right)+(\omega\tau_1)^{2(1-\alpha_1)}} + \frac{(\varepsilon_2-\varepsilon_\infty)(\omega\tau_2)^{1-\alpha_2}\cos\left(\frac{\alpha_2\pi}{2}\right)}{1+2(\omega\tau_2)^{1-\alpha_2}\sin\left(\frac{\alpha_2\pi}{2}\right)+(\omega\tau_2)^{2(1-\alpha_2)}} \quad (6)$$

By calculating $\varepsilon(\omega)$, refractive index and therefore scattering coefficient and path loss can be computed by Eqs. 7-8. Tables 2-3 show the required coefficients for calculation of Collagen Type-I and fat tissue's refractive indices, the coefficients are obtained by fitting the theoretical graphs to empirical ones.

$$\mu_{sca} = \rho_v Q_{sca}\sigma_g \quad (7)$$

$$PL_{sca} = e^{-\mu_{sca}d} \quad (8)$$

where in Eqs. 7-8, ρ_v =(volume fraction)/(volume of the particle), Q_{sca} is the scattering efficiency which equals ratio of scattering cross-section to geometrical cross-section, σ_g is the geometrical cross-section, μ_{sca} is the scattering coefficient, and PL_{sca} is scattering path loss in decibels at a certain distance of d.

Table 2: double Debye parameters of Collagen Type 1

ε_∞	ε_1	ε_2	$\tau_1(ps)$	$\tau_2(ps)$	Ref.
2.0	11.4	7.1	9.1	1.1	[15]

Table 3: double Cole-Cole parameters of Subcutaneous Fat

ε_∞	ε_1	ε_2	$\tau_1(ps)$	$\tau_2(ps)$	α_1	α_2	Ref.
1.3	9.0	5.0	0.9	4.01	0.45	0.1	[16]

The equation for calculation of scattering efficiency (Q_{sca}) differs based on the model. In the first case in which propagation of terahertz wave in air and its scattering as a consequence of interaction with fat tissue is considered, Mie model is used. However, in the second case which takes into account the propagation of terahertz waves in the collagen type I and its scattering as a consequence of collision with fat cells, Rayleigh-Gans-Born (RGB) model is used. The application of RGB model is because of low refractive index contrast between scatterer and its surrounding medium and also due to fat cell's size which satisfies the size parameter condition in Table 1. The scattering efficiency equations in Mie and Rayleigh-Gans-Born model for TE and TM polarization are shown in Eqs. 9-11 [14]. In Eq. 9, a_q and b_q are Mie coefficients with Bessel order of q (q=1, 2, …). Moreover, in Eq. 10-11, U = $4x$ and $\gamma = 0.577$ is the Euler's constant.

$$(Q_{sca})_{Mie} = \frac{2}{x^2}\sum_{q=1}^{\infty}(2q+1)\left(|a_q|^2 + |b_q|^2\right) \quad (9)$$

[Downloaded from ijop.ir on 2026-11-25]

$$((Q_{sca})_{RGB})_{TE} = (\mathrm{m}-1)^2\left\{-\frac{1}{4}-\frac{\sin(4\mathrm{x})}{8\mathrm{x}}-\right.$$
$$\left.-\frac{(1-\cos(4\mathrm{x}))}{32\mathrm{x}^2}+\mathrm{x}^2\right\} \quad (10)$$

$$((Q_{Sca})_{RGB})_{TM} = (\mathrm{m}-1)^2\left\{\frac{11}{4}+2\mathrm{x}^2-\right.$$
$$\frac{\sin(\mathrm{U})}{\mathrm{U}}-\frac{7}{16\mathrm{x}^2}(1-\cos(\mathrm{U}))+\left(\frac{1}{2\mathrm{x}^2}-2\right)\times$$
$$\left.\times\left(\gamma+\mathrm{Ln}(\mathrm{U})-\mathrm{Ci}(\mathrm{U})\right)\right\} \quad (11)$$

III. Simulation Results

The scattering path loss for the forearm's subcutaneous fat with the thickness of 1.65mm is calculated in the double-Debye's optimal frequency range (0.1-1 THz). Figure 1 and Fig. 2 demonstrates scattering coefficient and path loss for TE polarization. The same parameters are shown in Fig. 3 and Fig. 4 for TM polarization.

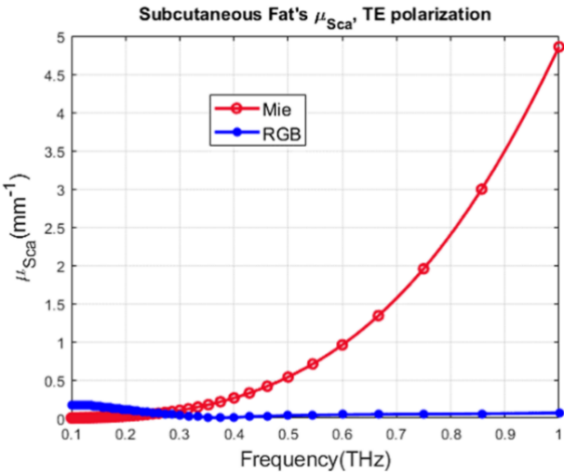

Fig. 1. Scattering coefficient in two conditions of air-enclosed (Mie) and tissue-enclosed (RGB) for TE Polarization.

From Figs. 1-2 it can be deduced that assuming air as the ambient can lead to a smaller and bigger scattering coefficient and path loss for frequencies below and above 0.26 THz. The biggest contrast between the models occurs at 0.38 THz in which a sharp deep is observable in the Rayleigh-gans-born model.

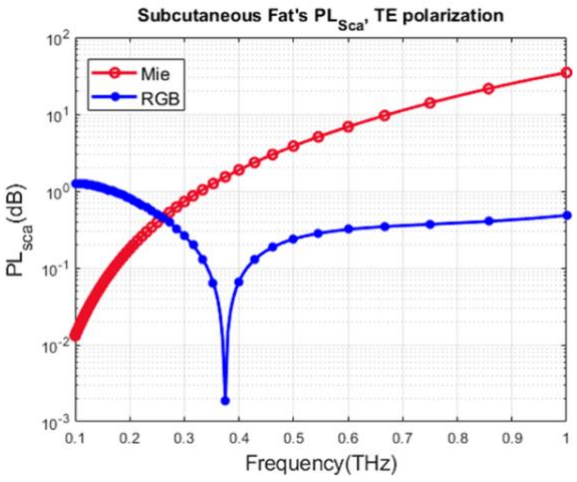

Fig. 2. Fat tissue's scattering path loss in air-enclosed (Mie) and tissue-enclosed (RGB) situations for TE Polarization.

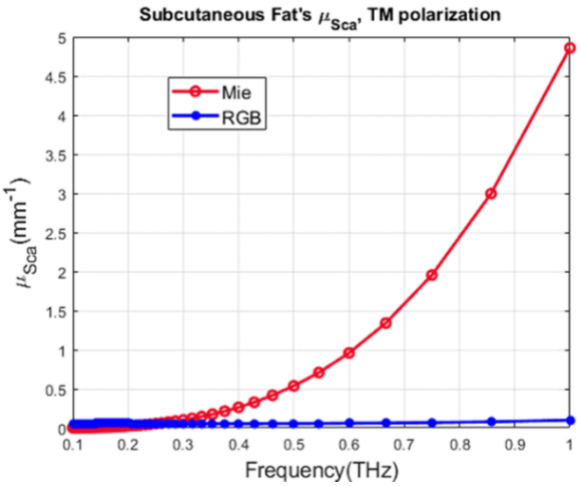

Fig. 3. Scattering coefficient of air-enclosed and tissue-enclosed conditions for TM polarization of fat tissue.

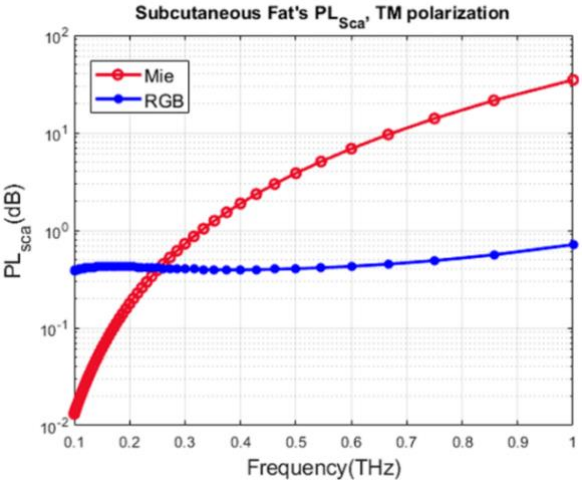

Fig. 4. Scattering path loss of fat tissue in two cases of air-enclosed and tissue-enclosed for TM polarization.

[Downloaded from ijop.ir on 2026-11-25]

In TM polarization as well, it can be seen from Figs. 3-4 that air-enclosed case causes bigger scattering for frequencies above 0.26 THz. However, in general, the behavior of scattering path loss and coefficient in two cases of air-enclosed and tissue-enclosed is closer in TM polarization compared to that of TE one.

IV. CONCLUSION

In this paper, the role of the surrounding medium in intra-body scattering for fat tissue is surveyed. In this regard, scattering of fat tissue in two scenarios of air-enclosed and tissue-enclosed scattering is calculated with Mie and Rayleigh-Gans-Born models respectively. In air-enclosed scattering, propagation of terahertz wave in the air and its scattering with fat tissue is considered whereas, in tissue-enclosed scattering, propagation of terahertz wave in fat tissue and its scattering as a consequence of collision with fat cells is studied. It is observed that assuming air as the surrounding medium leads to underestimation and overestimation of scattering loss in frequencies below and above 0.26 THz. Both models anticipate an equal amount of scattering loss in this frequency. Mie and Rayleigh-Gans-Born models show less contrast with TM polarization compared to TE polarization. The greatest difference between models occurs at approximately 0.4THz for TE polarization.

REFERENCES

[1] T. Robin, C. Bouye, and J. Cochard, *Terahertz applications: trends and challenges*, in Terahertz, RF, Millimeter, and Submillimeter-Wave Technology and Applications VII, San Francisco, 2014.

[2] Y. Peng, C. Shi, X. Wu, Y. Zhu, and S. Zhuang, "Terahertz imaging and spectroscopy in cancer diagnostics: a technical review," Am. Assoc. Adv. Sci., Vol. 2020, pp. 1-11, 2020.

[3] T. Amini, F. Jahangiri, Z. Ameri, and M.A. Hemmatian, "A Review of Feasible Applications of THz Waves in Medical Diagnostics and Treatments," Lasers. Med. Sci., Vol. 12, pp. e92 (1-8), 2021.

[4] M. Borovkova, M. Khodzitsky, P. Demchenko, O. Cherkasova, A. Popov, and I. Meglinski, "Terahertz time-domain spectroscopy for non-invasive assessment of water content in biological samples," Biomed. Opt. Express, Vol. 9, pp. 2266-2276, 2018.

[5] F. Lemic, S. Abadal, W. Tavernier, P. Stroobant, D. Colle, E. Alarcon, J. Marquez-Barja, and J. Famaey, "Survey on Terahertz Nanocommunication and Networking: A Top-Down Perspective," IEEE J. Sel. Areas Commun., Vol. 39, pp. 1506-1543, 2021.

[6] I.F. Akyildiz and J.M. Jornet, "Electromagnetic wireless nanosensor networks," Nano Commun. Networks, Vol. 1, pp. 3-19, 2010.

[7] N. Rikhtegar and M. Keshtgary, "A brief survey on molecular and electromagnetic communications in nano-networks," Int. J. Comput. Appl., Vol. 79, pp. 16-28, 2013.

[8] E. Lallas, "Key Roles of Plasmonics in Wireless THz Nanocommunications," Appl. Sci., Vol. 9, pp. 5488 (1-34), 2019.

[9] N. Saeed, M. Loukil, and H. Sarieddeen, "Body-centric terahertz networks: Prospects and challenges," IEEE Trans. Molec. Biolog. Multi-Scale Commun., Vol. 8, pp. 138-157, 2021.

[10] H. Elayan, R.M. Shubair, J.M. Jornet, and P. Johari, "Terahertz Channel Model and Link Budget Analysis for Intrabody Nanoscale Communication," IEEE Trans. NanoBioSci., Vol. 16, pp. 491-503, 2017.

[11] Z. Ameri and F. Jahangiri, "Effects of the surrounding medium on terahertz wave scattering loss in intrabody communication," Waves in Random and Complex Media, https://doi.org/10.1080/17455030.2022.2102266, pp. 1-15, 2022.

[12] J. Kindt and C. Schmuttenmaer, "Far-infrared dielectric properties of polar liquids probed by femtosecond terahertz pulse spectroscopy," J. Phys. Chem., Vol. 100, pp. 10373-10379, 1996.

[13] K. Cole and R. Cole, "Dispersion and absorption in dielectrics I. Alternating current characteristics," J. Chem. Phys., Vol. 9, pp. 341-351, 1941.

[14] V. D. Hulst, *Light Scattering by Small Particles*, New York: Dover Publication, 1981.

[15] R. Zhang, K. Yang, Q.H. Abbasi, N.A. AbuAli, and A. Alomainy, "Impact of cell density and collagen concentration on the electromagnetic properties of dermal equivalents in the

[Downloaded from ijop.ir on 2026-11-25]

terahertz band," IEEE Trans. Terahertz Sci. . Technol., Vol. 8, pp. 381-389, 2018.

[16] K. Sasaki, M. Mizuno, K. Wake, and S. Watanabe, "Measurement of the dielectric properties of the skin at frequencies from 0.5 ghz to 1 Thz using several measurement systems," 40th International Conference on Infrared, Millimeter, and Terahertz waves (IRMMW-THz), Hong Kong, 2015.



Zoha Ameri was born in Tehran. She received her B.S. degree in Engineering Physics from the Alzahra University, Tehran, Iran. In 2022, she received her M.S. degree in photonics. She is currently a Ph.D. candidate with interests in the fields of terahertz waves, wireless communications, and Body Area Nano-NETworks.



Fazel Jahangiri is an assistant professor of photonics at Laser and plasma research institute, Tehran, Iran.

He received his B.Sc. in Applied Physics from K.N. Toosi University of Technology in 2004, his M.Sc. in Photonics from Shahid Beheshti University in 2007 in Tehran and Ph.D. in Physics from Kyoto University, in 2012. His research interests include Terahertz science, Ultrashort laser pulses, Nonlinear optics, and Laser plasma interaction.

[Downloaded from ijop.ir on 2026-11-25]